Rev. Letters 27, 1463 (1971).
[4]P. Horvat, P. Kump, and B. Povh, Nucl. Phys. 45, 341 (1963).
[5]J. L. Durell, P. R. Alderson, D. C. Bailey, L. L. Green, M. W. Greene, A. N. James, and J. F. Sharpey-Schafer, J. Phys. A5, 302 (1972).
[6]P. W. M. Glaudemans, private communication.
[7]E. Sheldon and D. M. Van Patter, Rev. Mod. Phys. 38, 143 (1966).
[8]O. Häusser and N. Anyas-Weiss, Can. J. Phys. 46, 2809 (1968).
[9]J. F. Sharpey-Schafer, P. W. Ollerhead, A. J. Ferguson, and A. E. Litherland, Can. J. Phys. 46, 2039 (1968).

PHYSICAL REVIEW C VOLUME 6, NUMBER 2 AUGUST 1972

Isomer Ratios from Low Primary Excitation of Residual Nuclei*

J. W. Watson
Knolls Atomic Power Laboratory, Schenectady, New York 12301

and

H. A. Medicus and R. E. Turner
Department of Physics, Rensselaer Polytechnic Institute, Troy, New York 12181

(Received 28 February 1972)

A calculational procedure based on the Huizenga-Vandenbosch formalism for the determination of isomer ratios has been developed which is applicable also at low primary excitation energies of the residual nuclei, in contrast to earlier methods. This has been accomplished by introducing level densities which are based on the shell-model level calculations of Hillman and Grover rather than a level-density formula. Furthermore, the assumption that all the neutrons are emitted with the average energy $2T$ (where T is the nuclear temperature) has been replaced by a more realistic neutron spectrum. In order to test this procedure, the isomer ratio of Y^{87} from the photonuclear reaction $Y^{89}(\gamma, 2n)$, which has its reaction threshold at 20.8 MeV, was measured for bremsstrahlung of end-point energies 23, 25.6, 28.6, and 50 MeV. The results of our method are in much better agreement with the experiment than the original Huizenga-Vandenbosch approach. The analysis indicates that a relatively large fraction of the product nuclei is formed directly in the ground state and that quadrupole transitions are an important decay mode near the threshold.

I. INTRODUCTION

Isomer ratios yield useful information in regard to reaction mechanisms and the spin dependence of nuclear level densities. In these investigations the formalism developed by Huizenga and Vandenbosch,[1,2] has proven particularly successful. Whereas in many circumstances the simplifying assumptions of this method may lead to quite satisfactory results, there are also many instances where it is necessary to refine the original formalism in various respects.

The Huizenga-Vandenbosch approach presupposes that after the emission of the nucleons the product nuclei are initially formed, if not exclusively then at least predominantly, in relatively highly excited states, such that the level density of the final nucleus is large enough to justify a general statistical treatment. In many circumstances this condition of sufficient primary excitation energy of the product nucleus is easily satisfied, but there also exist types of reactions where this is not necessarily the case. In $(n, 2n)$ reactions with 14-MeV neutrons[3,4] for example, the residual nucleus is usually formed in states of relatively low excitation energy. Other examples are the bremsstrahlung-induced photonuclear reactions involving the emission of two nucleons. For this type of reaction, even if the end-point energy of the bremsstrahlung is appreciably higher than the threshold energy, most of the integrated yield will stem from the relatively narrow energy range of the photonuclear giant resonance.

In this paper, we will focus on $(\gamma, 2n)$ reactions. These reactions may be visualized as falling into three different classes, depending on the amount of primary excitation energy originally given to the final nucleus: The first class consists of the reactions in which after the emission of the two neutrons the ground state is reached directly. The second class comprises the reactions in which after the emission of the two neutrons the residual nucleus is reached in a state of small or moderate primary excitation energy up to 3 or 4

MeV. Finally, the third class is constituted by the reactions in which the residual nucleus is highly excited. The domain of validity for the usual Huizenga-Vandenbosch approach is restricted to this third class.

We have investigated the reaction $Y^{89}(\gamma, 2n)Y^{87}$, which leaves the final nucleus either in its ground state or in the isomeric state of 0.381 MeV. The angular momenta and parities of these two states are $\frac{1}{2}-$ and $\frac{9}{2}+$, respectively. The ground state of Y^{89} is $\frac{1}{2}-$, and the threshold for the $(\gamma, 2n)$ reaction is 20.8 MeV. According to Berman *et al.*,[5] whose data reach up to an energy of 28 MeV, and which are corroborated by measurements of Leprêtre *et al.*,[6] the giant resonance in yttrium has its maximum at 16.8 MeV, and its width at half maximum extends roughly from 15 to 19 MeV. The Lorentz fit through the giant resonance practically reaches zero at an energy of approximately 35 MeV. We assumed that likewise the $Y^{89}(\gamma, 2n)$ cross section tails off to that energy. This assumption is particularly justified because competition from the $(\gamma, 3n)$ reaction sets in at 33.8 MeV. In our experiment, the reactions were induced by thin-target bremsstrahlung with four different end-point energies between 23 and 50 MeV.

II. EXPERIMENTAL PROCEDURE

The isomer ratio in Y^{87} was determined by measuring the decay rates of the 381-keV isomeric transition and of the 485-keV γ ray which is emitted in the decay of the Y^{87} ground state (see Fig. 1). The half-lives of the isomeric transition and of the ground-state decay have recently been remeasured by Zoller, Walters, and Coryell[7] and were found to be 13.2 and 80.3 h, respectively. Twenty years ago, the conversion coefficient for the $M4$ isomeric transition was determined by Mann and Axel[8] as 0.28, a value which agrees reasonably well with the theoretical one of 0.24 given by Hager and Seltzer.[9] We assumed in our calculation a conversion coefficient of 0.26. 92.5% of the decays of the Y^{87} ground state proceed by way of a practically unconverted γ ray of 485 keV.

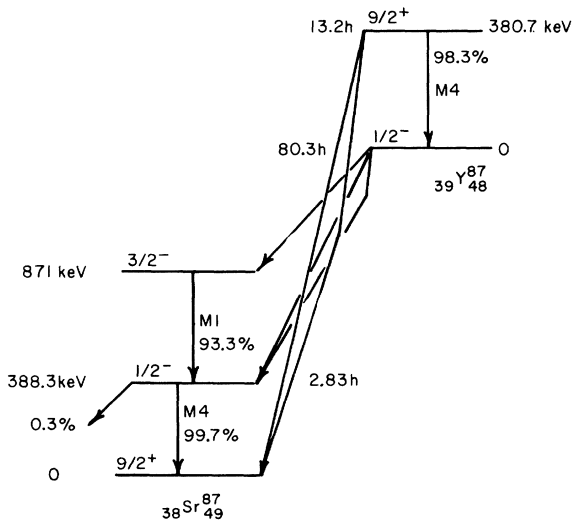

FIG. 1. Decay schemes of 13.2-h Y^{87m}, 80-h Y^{87g}, and 2.83-h Sr^{87m}.

Samples of approximately 4 g each of Y_2O_3 were irradiated at the Rensselaer electron linac with bremsstrahlung of end-point energies of 23, 25.6, 28.6, and 50 MeV. The bremsstrahlung was produced in a 10-mil-thick tungsten target. The energy spread of the electrons was approximately 3% (full width at half maximum), and the energy calibration was known to ±0.8 MeV. Each irradiation lasted for 1 h, with the exception of the 50-MeV run, which was of 20-min duration. Following this, the induced activity was measured with a Princeton-γ-Tech 25-cm^3 Ge(Li) detector. Its efficiency was determined with standard calibration sources in the relevant energy range. The resolution of the detector was sufficiently high to completely separate the 381-keV γ line from the 388-keV γ line which is emitted in the isomeric transition of Sr^{87}. This nuclide is the decay product of the Y^{87} decay, but it is also the product nucleus of the (γ, pn) reaction on Y^{89}.

Using the standard equations for radioactive decay and taking account of the finite irradiation time, the branching in the decay of the ground state, and the conversion coefficients, we arrived at the isomer yield ratios ($Yield_{metastable\ state}/Yield_{total}$) given in Table I.

III. ISOMER RATIO CALCULATIONS

A. Analytical Modifications of the Standard Procedure

Statistical calculations as they apply to the determination of isomer ratios have been discussed in detail by a number of authors.[1,2,10-15] In our calculations, however, we do not use two of the limiting approximations usually made in calculating the broadening of the spin distribution in the course of the deexcitation:

(1) The level-density formulas usually employed in such calculations are replaced by discrete levels whose energies and angular momenta have been calculated by Hillman and Grover[16] with a shell-model combinatorial method.

(2) The simplifying assumption that neutrons of average energy $2T$ (where T is the nuclear tem-

TABLE I. Experimental isomer ratios: $Y^{89}(\gamma,2n)Y^{87m},Y^{87g}$.

Bremsstrahlung end-point energy (MeV)	Measured isomer ratio Metastable state/total
23.0 ± 1.5	0.2 ± 0.02
25.6 ± 1.5	0.26 ± 0.025
28.6 ± 1.6	0.30 ± 0.03
50.0 ± 2.3	0.35 ± 0.03

perature)[1,2] will represent the effect of the actual emitted neutron spectrum has been dropped. Instead, energy spectra are computed for the emitted neutrons using evaporation theory. The level densities required for these calculations are derived from Hillman and Grover's calculations. Although these refinements are especially important at low excitation energies, comparisons by Hillman and Grover[16] between the usual level-density formulas and their shell-model calculations indicate that misleading trends in the algebraic formulation for the spin distribution may persist up to relatively high excitations (~11 MeV). It should be noted, however, that the deviations at higher energy become pronounced particularly for higher angular momenta. Therefore, they are of less significant influence in photonuclear reactions which have characteristically narrow spin distributions.

For our experiment the relevant range of the excitation energy of the target nucleus is represented by the energies 22, 23, 24, 25, 26, 28, and 30 MeV. Associated with each of these energies are angular momenta of $\frac{1}{2}$ and $\frac{3}{2}$ corresponding to dipole transitions by the photonuclear absorption process since the angular momentum of the ground state of the target nucleus is $\frac{1}{2}$. The subsequent deexcitation and broadening of the spin distribution is shown schematically in Fig. 2 and is discussed below.

There are many different decay paths between a pair of distinct levels in the excited target nucleus and in the final nucleus in its primary excited state, i.e., the state from which the γ-deexcitation cascade begins, because a great number of intermediate states in Y^{88} can be reached by the emission of the first neutron. Hillman furnished us with a listing of levels by spin in 0.5-MeV energy bins in Y^{88} and 0.3-MeV bins in Y^{87}. Our computer program was set up to evaluate the relative probabilities of all energetically possible decay paths between a level of given energy and spin in Y^{89} and a level of specific spin at the center of an energy bin in Y^{87}. For transitions starting from the relatively low excitation energies of 23, 24, and 25 MeV in Y^{89} the energy bins in Y^{88} were subdivided further by linear interpolation into 0.1- or 0.25-MeV intervals to obtain a better representation of the neutron spectrum. Such calculations were done for each spin in a bin of Y^{87} and for each energy bin. Hereafter the procedure was repeated for the second possible angular momentum value of the dipole state in Y^{89}. In the same manner all transitions to the bins in Y^{87} which originate from the seven representative excited levels in Y^{89} were processed by the computer program.

In the neutron-emission stages, the relative populations of various possible final spin states depend on the neutron energy, the barriers for the various orbital angular momenta, and the spin dependence of the level density. In our calculations we used Auerbach and Perey's[17] optical-model transmission coefficients. Isospin effects were neglected in our calculation.

The shell-model level densities for Y^{88} and Y^{87} were introduced as two-dimensional data arrays in spin and energy. For each deexcitation phase the appropriate level-density information was selected from the table taking into account the residual energy of the particular reaction channel and the range of spins allowed by the relevant angular momentum selection rules.

The combinatorial technique employed by Hillman and Grover[16] defines a set of level densities dependent upon a pairing-force parameter G. In our case, since neutron-resonance data for Y^{88}

TABLE II. Y^{87} level-density table. Lowest 23 levels.

	Before modification No. of levels						After modification No. of levels				
Energy (MeV)/Spin	$\frac{1}{2}$	$\frac{3}{2}$	$\frac{5}{2}$	$\frac{7}{2}$	$\frac{9}{2}$	Energy (MeV)/Spin	$\frac{1}{2}$	$\frac{3}{2}$	$\frac{5}{2}$	$\frac{7}{2}$	$\frac{9}{2}$
0.0–0.3	1	0	0	0	1	0.0–0.380	1	0	0	0	0
0.3–0.6	0	0	0	0	0	0.381–0.6	0	0	0	0	1
0.6–0.9	2	0	0	0	0	0.6–0.9	2	0	0	0	0
0.9–1.2	0	0	0	0	0	0.9–1.2	0	0	0	0	0
1.2–1.5	2	3	4	5	5	1.2–1.5	2	3	4	5	5

and Y^{87} were not available, this parameter was varied so as to obtain agreement with the level densities determined from experimental neutron-resonance data of neighboring nuclides. This procedure yields $G = 11/A$ for Y^{88} and $G = 10.3/A$ for Y^{87}. To further assure consistency with existing experimental data, the Y^{87} level-density data were rearranged in the lowest four levels to explicitly represent the lowest known experimental levels in Y^{87}. This is shown in Table II.

Hillman and Grover have noted that near closed neutron shells an anomalous variation occurs in the pairing-force parameter G which is required to fit the resonance data. However, closer examination of their data indicates that this effect is quite weak in the neighborhood of the $N = 50$ neutron shell which is filled in Y^{89}.

After the emission of the second neutron the subsequent γ cascade is assumed to consist of dipole transitions with exception of the last step. The energy of the cascade γ rays was estimated from the empirical formula of Vonach, Vandenbosch, and Huizenga[18] to be

$$E_\gamma = 4(E/a - 5/a^2)^{1/2},$$

where E_γ is the γ energy in MeV, E is the excitation energy in MeV, and a is the level-density parameter as determined by Gilbert and Cameron.[19]

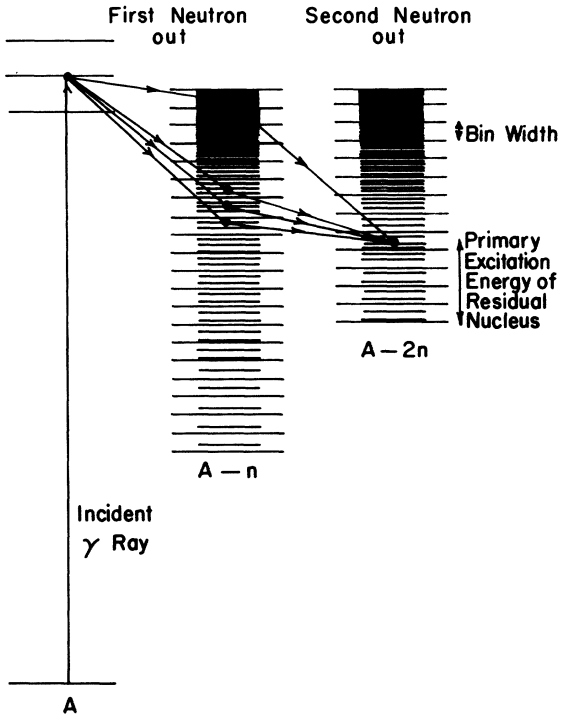

FIG. 2. Representative decay paths leading from a level in the target nucleus to a level of primary excitation energy in the residual nucleus.

The average number of cascade γ rays in a particular reaction channel thus depends on the available energy. When the excitation energy finally became so low that another dipole γ ray of the prescribed energy would lead to an energy below that of the isomeric level, a transition was instead assumed that would lead either to the isomeric or to the ground state, whichever required the smaller change in angular momentum. Thus, the number of γ rays varied with the individual reaction channel and was not a model parameter as in some of the previous work on isomer ratios.

This explicitly defined spectrum of reaction channels is then sequentially processed through the spin-broadening computations, each resulting in a spin redistribution unique to that channel.

All the possible decay paths which start from levels of the previously mentioned seven excitation energies in the region in which the $(\gamma, 2n)$ cross section is important were treated in this same way. This yielded for each excitation energy of Y^{89} an isomer ratio in Y^{87}. In order to compare the calculated results with our experimental ones, each decay path was weighted with the shape of the bremsstrahlung spectrum and the energy dependence of the $(\gamma, 2n)$ cross section.

B. Computational Details

For each channel, a reaction-rate weighting factor is computed in the following way: For an initial state of spin J_C, the relative probability R for emitting a particle of energy ϵ and leading to another state of spin J_f and residual energy E_R is assumed to be, analogous to Ref. 15,

$$R(\epsilon, E_R, J_\rho)_{J_C} \propto \epsilon \rho(J_f, E_R) \sum_{S=|J_f - s'|}^{J_f + s'} \sum_{l'=|J_C - S|}^{J_C + S} T_{l'}(\epsilon),$$

where s' is the intrinsic spin of the emitted particle, S is the channel spin, $T_{l'}(\epsilon)$ is the transmission coefficient of the emitted particle with angular momentum l' and energy ϵ, and $\rho(J_f, E_R)$ is the level density. By summing this quantity over all final spin states, one obtains a relative measure of the reaction rate P for this particular emission energy, i.e.,

$$P(\epsilon, E_R) \propto \sum R(\epsilon, E_R, J_f),$$

where the sum is to be taken in the case of $J_C - l_{\max} - s' \leq 0$ from $J_f = J_{fI}$ to $J_f = J_C + l'_{\max} + s'$, and in the case of $J_C - l'_{\max} - s' > 0$ from $J_f = J_C - l'_{\max} - S$ to $J_f = J_C + l'_{\max} + s'$. J_{fI} is the initial value of the index J_f. If the maximum value of J_f is integer then $J_{fI} = 0$, and if half integer then $J_{fI} = \frac{1}{2}$.

For the multiple-particle emission of our analysis, the product $P(\epsilon_1, E_{R1}) \times P(\epsilon_2, E_{R2})$ was formed

and served as the reaction-rate weighting factor for individual-channel isomeric yield fractions.

The cascading of dipole γ rays was considered terminated when the next γ transition would drop the residual energy below the isomeric level (0.381 MeV), as described previously. At this point the fraction of the yield to the isomeric state for the channel under consideration was computed directly from the accumulated yield fractions. For those channels where some of the yield was stranded at the $\frac{5}{2}$-spin state and only $\frac{1}{2}$ and $\frac{9}{2}$ levels remained which are unattainable by dipole emission, the $\frac{5}{2}$-state yield fraction was equally divided between $\frac{1}{2}$- and $\frac{9}{2}$-spin states.

The isomer ratio was calculated for monoenergetic photons at representative energies and the effects of the bremsstrahlung spectrum were folded into the isomer-ratio calculations by computing the relative intensity of the $(\gamma, 2n)$ reactions resulting from various bremsstrahlung energies. This was directly possible using the experimental $(\gamma, 2n)$ cross section $\sigma_{2n}(E_\gamma)$ determined for Y^{89} by Berman *et al.*[5] Appropriate weighting factors normalized to the experimental yield were derived for the ith bin as

$$P_{\gamma i} = \frac{\int_{E_{\gamma i}}^{E_{\gamma(i+1)}} \varphi(E_\gamma, E_0)\sigma_{2n}(E_\gamma)dE_\gamma}{\int_{E_{\gamma\,\text{threshold}}}^{E_0} \varphi(E_\gamma, E_0)\sigma_{2n}(E_\gamma)dE_\gamma},$$

where $\varphi(E_\gamma, E_0)$ is represented by a Schiff bremsstrahlung spectrum for the thin-target irradiations of this experiment.

IV. RESULTS

The isomer yield fraction occupying the high-spin $(\frac{9}{2})$ state was calculated for monoenergetic photons of 22, 23, 24, 25, 26, 28, and 30 MeV. These results are presented in Fig. 3. Inclusion of the bremsstrahlung spectral shape resulted in a theoretical yield fraction which together with our experimental data is shown in Fig. 4. The experimental results are also presented in Table I. Above 28 MeV agreement is quite good, although the calculated values are low by 10 to 15%. Below 28 MeV down to threshold (20.8 MeV) there is an increasing discrepancy on the same side.

Quadrupole transitions in the γ cascade have not been considered in the above results, but it is known, for example, from the work of Sperber and Mandler,[14] that they can modify the isomer ratio. Quadrupole transitions, in general, tend to equalize the populations of the two states in question in comparison to pure dipole transitions. In our case they will therefore increase the high-spin yield fraction. An upper limit to the magnitude of this effect was estimated by assuming γ cascades consisting only of quadrupole transitions and by using the same calculated spin distribution as before. As in the calculations for dipole cascades, parity considerations have been neglected. The results for this hypothetical case of quadrupole transitions only are shown as a dashed line in Fig. 4. It is noteworthy that agreement with the experimental data will be markedly improved at energies near threshold if quadrupole transitions are included.

Another study concerned the influence of additional levels. It is clear that the levels calculated by Hillman, although an improved approximation, will only roughly represent the actual situation, especially at the lowest energies. In order to obtain an estimate of how much an additional level might change the isomer ratio, a level of spin $\frac{7}{2}$ situated in the energy band from 0.381 to 0.9 MeV was added. The results of our calculation are presented in Table III. As would be expected, the largest effects are seen near the reaction thres-

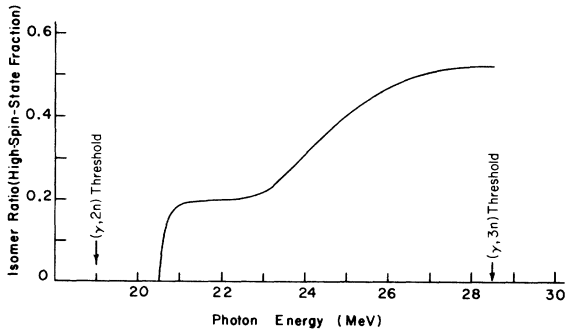

FIG. 3. Calculated isomer ratio in Y^{87} from the reaction $Y^{89}(\gamma, 2n)Y^{87}$ vs photon energy. Pure dipole cascades are assumed.

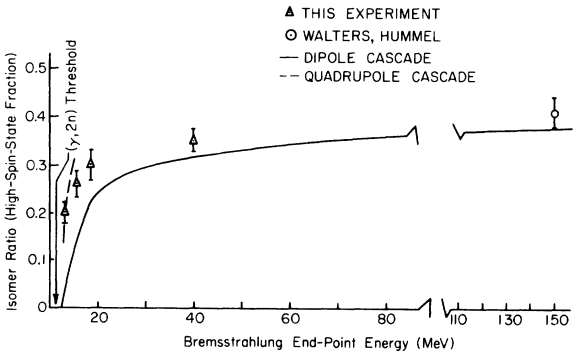

FIG. 4. Isomer ratio in Y^{87} from the reaction $Y^{89}(\gamma, 2n)$-Y^{87} vs end-point energy of thin-target bremsstrahlung.

hold, and they diminish at higher energies as neutron emissions of higher angular momenta and multiple γ transitions become more probable.

In order to obtain some clues to how systematic errors in the energy determination of the levels by Hillman and Grover's method might influence the calculated isomer ratio, we shifted the energy of each bin containing a certain level density downward by 0.2 MeV. This energy shift reduced the isomer ratio for 23-MeV end-point bremsstrahlung by about 10% but had negligible effects for higher energies.

In recent investigations Maher, Comfort, and Morrison[20] have experimentally determined a number of levels in Y^{87} up to 3.6 MeV by single-proton stripping from (He^3, d) reactions. A comparison of their findings with the shell-model calculations of Hillman are shown in Table IV. The selective nature of stripping reactions does not give an account of all available levels, missing in particular many with higher spins. On the other hand, a few levels are indicated which were not predicted at that energy location by the shell-model calculations. Relatively important is an $f_{5/2}$ level at 0.793 MeV, which therefore falls into the 0.6–0.9-MeV band. The introduction of this level would influence our results in a manner similar to that calculated with an additional $\frac{7}{2}$ level, as discussed above.

Since the quoted experimental data do not include many levels of higher spin, use of these data alone would further enhance the ground-spin-state population and increase the discrepancy between the calculated and the experimental isomer yield results. Clearly, for our purposes the levels known from experiments give an insufficient description of the complete spin distribution. The levels from shell-model calculations are much more suitable, even though the energy distributions may be somewhat shifted depending on the nuclear potentials assumed.

V. DISCUSSION

We consider first the case of a photonuclear reaction which is induced by a monoenergetic photon beam (for example from positron annihilation in flight). Later we shall discuss the results due to the continuous bremsstrahlung spectrum which were actually obtained in our experiment. The first phase of our reaction, the excitation of the target nucleus, is quite simple since a dipole absorption is assumed and the target angular momentum is $\frac{1}{2}$. This results in a spin distribution in the excited nucleus which is 0.333 in the spin-$\frac{1}{2}$ state and 0.667 in the spin-$\frac{3}{2}$ state. We can assume that the reaction proceeds via a compound nucleus. Direct photonuclear reactions of the type (γ, $2n$) are rare and can be neglected. From these dipole states, neutron spectra are emitted. Figure 5 shows the resultant spin and energy distribution of the states in Y^{87} which are reached after emission of two neutron spectra assuming an initial excitation of 26 and 23 MeV in Y^{89}, respectively. Therefore, these initial excitation energies are 5 and 2 MeV, respectively, above the (γ, $2n$) reaction threshold. In the second case a more complex situation can be expected which is a consequence of the discrete level structure near threshold energy. It is also seen that the neutron emissions do not give rise to a strong broadening of the spin distribution because the centrifugal barriers impede the emission of neutrons of large angular momentum. This results in a preferential population of the spin states closest to the compound-nucleus spin states, which in this case are the $\frac{1}{2}$ and $\frac{3}{2}$ states. Since the ground state of Y^{87} has spin $\frac{1}{2}$, obviously it will be populated more strongly than the isomeric state with a spin of $\frac{9}{2}$. This is thus a fine example of the old observation that the state with a spin closer to the spin of the target nucleus will generally be the more populated one.

An additional factor favoring the population of the ground state is the energy difference of 0.381 MeV between the ground state and the isomeric

TABLE III. Effect of an additional $\frac{7}{2}$-spin level in the 0.381- to 0.9-MeV band.

Photon energy (MeV)	High-spin yield fraction Without $\frac{7}{2}$ state	With $\frac{7}{2}$ state
23.0	0.018	0.039
25.6	0.125	0.152
28.6	0.225	0.248

TABLE IV. Comparison of the shell-model calculations with known experimental levels.

Energy band (MeV)/Spin	Shell-model levels/experimental levels $\frac{1}{2}$	$\frac{3}{2}$	$\frac{5}{2}$	$\frac{7}{2}$	$\frac{9}{2}$
0.0–0.3	1/1	0/0	0/0	0/0	1/0
0.3–0.6	0/0	0/0	0/0	0/0	0/1
0.6–0.9	2/0	0/0	0/1	0/0	0/0
0.9–1.2	0/0	0/1	0/1	0/0	0/0
1.2–1.5	2/0	3/0	4/0	5/0	5/0
1.5–1.8	2/0	1/0	2/0	2/0	3/1
1.8–2.1	2/0	1/0	2/0	2/0	3/1
2.1–2.4	2/0	1/0	3/2	3/0	5/1
2.4–2.7	2/0	1/0	1/1	3/0	4/0
2.7–3.0	18/0	32/0	43/0	54/0	59/0
3.0–3.3	6/1	5/0	7/3	8/0	9/0
3.3–3.6	26/0	47/0	68/2	86/0	100/0

state, because the threshold to reach the latter is higher. It also has to be considered that neutrons need at least 1.1-MeV energy to overcome the centrifugal barrier to reach the $\frac{9}{2}-$ isomeric level. All this results in an effective threshold for the population of this state which is approximately 1.5 MeV higher than the $(\gamma, 2n)$ reaction threshold for the ground state.

It is obvious from the above that the distribution of the states in Y^{87} which are populated directly after the emission of the second neutron depends strongly on the energy of the absorbed photons. As the photon energy increases, there is a shift towards higher excitation energies of the residual nucleus. This is clearly seen in Fig. 6 in which are plotted the population fractions of the computed states in Y^{87} assuming initial dipole absorption in Y^{89} of 23-, 24-, 25-, and 26-MeV monochromatic photons. The conspicuous gap between 0.9 and 1.2 MeV is due to the fact that in Hillman's table no energy levels are listed here. Since the residual energy distributions are in the region below 4 MeV, it is apparent that the usual statistical-model assumptions are inappropriate for these initial excitations. The calculated isomeric-state yield fraction for increasing monoenergetic photon energies shown in Fig. 3 reflects all the points made in the previous discussion.

If bremsstrahlung is used to induce the reaction, as is here the case, rather than the monochromatic photon beam discussed above, the lower residual excitation energies are enhanced because of the shape of the bremsstrahlung spectrum. When the $(\gamma, 2n)$ reactions on Y^{89} are induced by 47-MeV bremsstrahlung, 15% of the reactions lead directly to the ground state of Y^{87}, without any γ emission. This fraction comprises the first class of reactions, as we mentioned in the Introduction. In 83% of the reactions, levels below 4.0-MeV excitation energy are reached following the emission of the second neutron. This is the second class of reactions, leaving the final nucleus in an energy region where the level structure cannot be reproduced by a level-density formula. In only about 2% of the reactions, which form the third class, is the primary excitation high enough that the usual Huizenga-Vandenbosch formalism could be justified.

An increasing high-spin-state yield fraction may be expected as the bremsstrahlung spectral distribution shifts to higher average energies because the average number of γ rays in the cascades in-

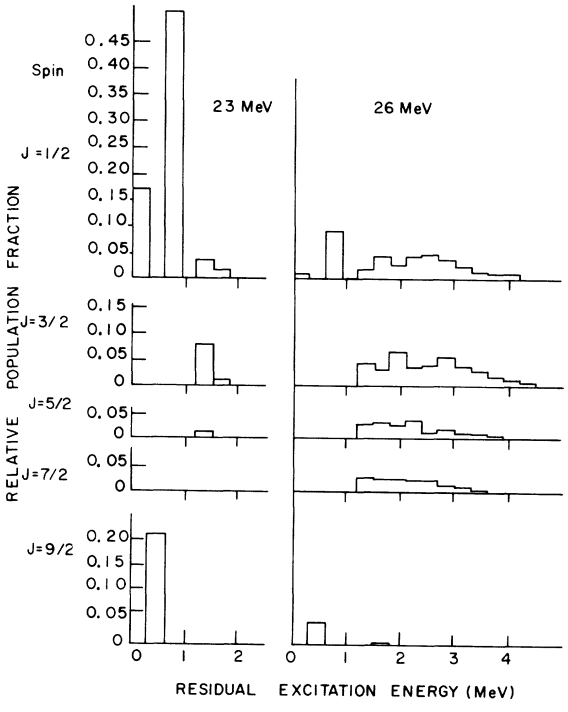

FIG. 5. Relative spin distributions in Y^{87} immediately after the emission of two neutrons from Y^{89} which has been excited by a 23- or 26-MeV γ ray. The spin distributions are shown for different primary excitation energies.

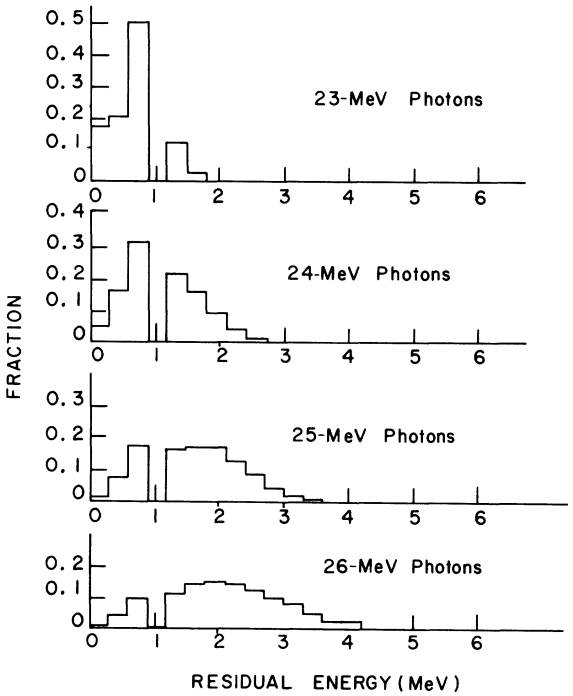

FIG. 6. Energy distribution of the residual Y^{87} nucleus in its primary excitation state following the emission of the second neutron.

creases and therefore also the broadening of the spin distribution towards the bottom of the cascades. However, the negligible $(\gamma, 2n)$ cross section above 35 MeV would indicate an asymptotic isomer-yield-fraction behavior for higher end-point energies because the spectral distribution over the energy range of significant $(\gamma, 2n)$ cross section, namely from 21 to 35 MeV, becomes less and less dependent on the bremsstrahlung end-point energy. Our data show this asymptotic behavior and are consistent with identical Y^{89}-$(\gamma, 2n)Y^{87}$ isomer ratios of 0.42 ± 0.03 measured at both 150- and 280-MeV end-point energies by Walters and Hummel.[21]

Isomer-ratio calculations with the original Huizenga-Vandenbosch approach were also made by Walters and Hummel, assuming an effective average photon energy of approximately 30 MeV which was determined from estimated $(\gamma, 2n)$ cross sections and the bremsstrahlung spectrum in their experiment. For reasonable values of the spin-cutoff parameter their calculations are generally in satisfactory agreement with their experimental data. Our results would indicate that the statistical approach of Huizenga and Vandenbosch becomes a useful approximation for average initial excitations greater than ~6 MeV above threshold (average photon energy greater than ~27 MeV for our reaction), but that this approach will fail to an increasing degree below this level and results in a spin-cutoff parameter σ between 1 and 2 which is much too low a value. Conversely, a realistic spin-cutoff parameter for yttrium of $\sigma = 3.5$ would produce a much too big isomer ratio of 0.4 to 0.5. A similar difficulty of this nature was reported by Slivinsky and Winter[22] for the (p, n) reaction on Sr^{87} with protons between 3.45 and 6.05 MeV which gave rise to residual-nucleus excitations between 0.75 and 3.35 MeV. It resulted in unreasonably small values for σ, which is consistent with the considerations presented here.

We find the greatest disagreement between our calculations and the experiment in the region of lowest energy, that is, below approximately 30-MeV bremsstrahlung end-point energy. It should be kept in mind that for our main calculation only deexcitations by dipole-radiation cascades were assumed. However as discussed earlier, the inclusion of quadrupole transitions may improve the agreement considerably. It is therefore suggestive that quadrupole transitions play an important role in the deexcitation process at lower energies. Sperber and Mandler[14] have found that quadrupole admixtures of 10 to 20% are required for the interpretation of experimental (n, γ) isomer ratios. In another paper, Liggett and Sperber[23] found in an evaluation of isomer ratios in Y^{87} produced by $(p, 2n)$ and $(\alpha, 2n)$ reactions optimum agreement by assuming 26% quadrupole radiation. This magnitude is consistent with the 10–15% deviation of our calculations for bremsstrahlung end-point energies above 30 MeV.

In our calculation we assumed a pure dipole excitation of the Y^{89} nucleus. A certain amount of quadrupole contribution to the giant resonance should not be ruled out, and it could be relatively strong at the high-energy wing of the resonance, the region in which most of the $(\gamma, 2n)$ cross section falls. Because quadrupole transitions can reach also the $\frac{5}{2}$ states in Y^{89}, one might surmise that they enhance somewhat the population of the isomeric $\frac{9}{2}$ state in Y^{87}. However, our calculations to this behalf showed that any reasonable amount of quadrupole contribution has surprisingly little effect on the isomer ratio at the low excitation energies where the discrepancy between experiment and theory is considerable.

One might ask if a better agreement between calculation and experiment might be obtained if nonequilibrium contributions to the neutron spectra were not neglected. It is known[24] that direct (γ, n) reactions will result in isomer ratios which are different from those from evaporation reactions. Presumably this will also be the case, although to a lesser degree for other nonequilibrium (γ, n) reactions. There is, however, very little reason to assume that nonequilibrium $(\gamma, 2n)$ reactions have a noticeable effect on the isomer ratio, since Berman *et al.* data (Fig. 3 of their paper) indicate constancy or even a slight drop in the average neutron energy from the $(\gamma, 2n)$ threshold on.

It should not be too surprising that at very low energies Hillman and Grover's calculated levels will not yield a completely correct isomer ratio because they predict only approximately the energy of the levels. At the low energies where only a few levels are involved, a quite detailed knowledge of the energy, spin, and parity of the levels is necessary for arriving at the correct ratio. The $(\gamma, 2n)$ reaction on Y^{89} of our experiment represents a severe test for isomer-ratio calculations because the shape and position of the giant dipole resonance, the very high reaction threshold, and the shape of the bremsstrahlung spectrum favor very low primary excitations in Y^{87}.

Our work bears some similarity to that of Pönitz[12] and Liggett and Sperber,[23] who also recognized that low-lying discrete levels influence the isomer ratio and therefore explicitly should be taken into account. Both groups incorporated into their computations the experimentally determined levels. However, by proceeding in this way one cannot be sure beforehand that the known levels are a reasonably fair representation of all low-

lying levels in that energy region and therefore will improve the calculation. Pönitz found in the case of Dy^{165} that when 20 known low-lying levels were taken into account, the agreement between the experimental and calculated isomer ratio became considerably worse in comparison with the usual method of taking only the ground and isomeric state. This is perhaps similar to the situation in Y^{87} where the experimental known levels, as mentioned earlier, represent the spin distribution of the levels in a very distorted fashion. From the investigations of Liggett and Sperber it appears that those levels with a spin value outside the range between the isomeric and the ground-state spin have a particular influence on the isomer ratio. If such levels are missed in an experimental determination, the inclusion of other levels may not improve the calculated isomer ratio. Our method which is based on calculated levels (whose energy might be adjusted slightly whenever possible) seems, therefore, to have a wider field of practical application. In a situation like ours, where nearly all of the γ cascades start in the region of discrete levels it is probably the only useful one.

Another difference between our method and the other two of Refs. 11 and 22 is in the treatment of the continuum region where we still use calculated levels instead of level-density formulas. This was done by us only for convenience because it eliminated automatically the problem of handling the transition from the continuum region to the region of discrete levels. Since the computer time involved in calculating the enormous number of levels at higher energy is considerable, a transition to a level-density formula at high energy would seem a valid and practical solution.

ACKNOWLEDGMENTS

We are most grateful to M. Hillman for furnishing us with a listing of the calculated energy levels for Y^{88} and Y^{87}. We also wish to thank D. Sperber for valuable discussions and the linac operating staff for its cooperation during the irradiation. The help in the early stages of the experimental work of Maria Rosia Van Nieuwenhuysen and James E. Bond is gratefully acknowledged.

---

*Work supported in part by the U. S. Atomic Energy Commission and by the National Science Foundation.

[1]J. R. Huizenga and R. Vandenbosch, Phys. Rev. 120, 1305 (1960).

[2]R. Vandenbosch and J. R. Huizenga, Phys. Rev. 120, 1313 (1960).

[3]J. Karólyi, J. Crikai, and G. Peto, Nucl. Phys. A122, 234 (1968).

[4]M. Guidetti and D. Oldans, Nucl. Phys. A152, 387 (1970).

[5]B. L. Berman, J. T. Caldwell, R. R. Harvey, M. A. Keeley, R. L. Bramblett, and S. C. Fultz, Phys. Rev. 162, 1098 (1967).

[6]A. Leprêtre, H. Beil, R. Bergère, P. Carlos, and A. Veyssière, Nucl. Phys. A175, 609 (1971).

[7]W. H. Zoller, W. B. Walters, and C. D. Coryell, Phys. Rev. 185, 1537 (1969).

[8]L. G. Mann and P. Axel, Phys. Rev. 84, 221 (1951).

[9]R. S. Hager and E. C. Seltzer, Nucl. Data A4, 1 (1968).

[10]R. Vandenbosch, L. Haskin, and J. C. Norman, Phys. Rev. 137, B1134 (1965).

[11]J. R. Grover, Phys. Rev. 123, 267 (1961).

[12]W. P. Pönitz, Z. Physik 197, 262 (1966).

[13]D. Sperber, Nucl. Phys. A90, 665 (1967).

[14]D. Sperber and J. W. Mandler, Nucl. Phys. A113, 689 (1968).

[15]W. L. Hafner, J. R. Huizenga, and R. Vandenbosch, ANL Report No. ANL-6662, 1962 (unpublished).

[16]M. Hillman and J. R. Grover, Phys. Rev. 185, 1303 (1969).

[17]E. H. Auerbach and F. J. Perey, BNL Report No. BNL 765 T-286, 1962 (unpublished).

[18]H. K. Vonach, R. Vandenbosch, and J. R. Huizenga, Nucl. Phys. 60, 70 (1964).

[19]A. Gilbert and A. G. W. Cameron, Can. J. Phys. 43, 1449 (1965).

[20]J. V. Maher, J. R. Comfort, and G. C. Morrison, Phys. Rev. C 3, 1162 (1971).

[21]W. B. Walters and J. P. Hummel, Phys. Rev. 150, 867 (1966).

[22]S. H. Slivinsky and R. G. Winter, Bull. Am. Phys. Soc. 12, 1042 (1967).

[23]G. Liggett and D. Sperber, Phys. Rev. 3, 447 (1971).

[24]J. R. Tatarczuk and H. A. Medicus, Phys. Rev. 143, 818 (1966).